J. Fluid Mech. (1999), *vol.* 386, *pp.* 127–148. Printed in the United Kingdom

Self-lubricated transport of bitumen froth

By DANIEL D. JOSEPH[1], RUNYAN BAI[1], CLARA MATA[1], KEN SURY[2] AND CHRIS GRANT[2]

[1] Department of Aerospace Engineering and Mechanics, University of Minnesota, Minneapolis, MN 55455, USA
[2] Syncrude Ltd, Edmonton Research Centre, Edmonton, Alberta T6N 1H4, Canada

(Received 29 December 1997 and in revised form 30 November 1998)

Bitumen froth is produced from the oil sands of Athabasca using the Clark's Hot Water Extraction process. When transported in a pipeline, water present in the froth is released in regions of high shear, namely at the pipe wall. This results in a lubricating layer of water that allows bitumen froth pumping at greatly reduced pressures and hence the potential for savings in pumping energy consumption. Experiments establishing the features of the self-lubrication phenomenon were carried out in a 25 mm diameter pipeloop at the University of Minnesota, and in a 0.6 m diameter pilot pipeline at Syncrude, Canada. The pressure gradient of lubricated flows in 25 mm, 50 mm and 0.6 m diameter pipes closely follow the empirical law of Blasius for turbulent pipe flow; the pressure gradient is proportional to the ratio of the $\frac{7}{4}$th power of the velocity to the $\frac{5}{4}$th power of the pipe diameter, but the constant of proportionality is about 10 to 20 times larger than that for water alone. We used Reichardt's model for turbulent Couette flow with a friction velocity based on the shear stress acting on the pipe wall due to the imposed pressure gradient to predict the effective thickness of the lubricating layer of water. The agreement with direct measurements is satisfactory. Mechanisms for self-lubrication are also considered.

1. Introduction

Recently, Syncrude Canada announced that its proposed Aurora Mine Project would extract bitumen froth from an oil sand lease located about 35 km from the upgrading plant at Mildred lake in Northern Alberta. One possible way of shipping bitumen froth from the remote extraction site to the current operations is pipelining in core–annular flow mode. Significant information exists in the literature on bitumens to which water is added as a lubricant (see Joseph & Renardy 1992 or Joseph *et al.* 1997), but no literature exists on self-lubrication.

Fouling of pipe walls is possibly the main impediment to the successful application of water-lubricated pipelining. It is desirable to lubricate the oil core with as little water as possible to alleviate the problem of dewatering. On the other hand, oil is more likely to foul the pipe wall when a small amount of water is used. The lubricated configuration with water on the wall is hydrodynamically stable. The water, the low-viscosity constituent, always migrates to the places where the shear rate is high: to the pipe wall. However, it is inevitable that the waves which levitate core flows off the wall will actually touch the pipe wall from time to time. If the wall is oleophilic, the oil will stick to it even though water near the wall is hydrodynamically stable; the carbon steels generally used for pipes are oleophilic and typically are fouled by oil. The fouling of pipe walls by oil may lead to a continual increase of the

pressure gradient required to drive the flow. A water annulus can lubricate an oil core even in a pipe whose walls are spotted with oil. Sometimes, however, the fouling builds up, leading to rapidly increasing pressure drops, and even blocking of the flow. The fouling buildup is especially pronounced for heavy crudes with high asphaltene content like Zuata crudes from the Orinoco belt (see Joseph *et al.* 1997).

Fouling is more pronounced near pumping stations, where the pressure is highest and the holdup ratio (the ratio of the average velocity of oil to the velocity of water) and core wave structure are developing, or around line irregularities such as unions, bends, flanges and curves. Another major problem could be an unexpected shut-down in the line; the oil and water would stratify, causing the oil to stick to the pipe wall, making it harder to restart the line.

Although No. 6 fuel oil routinely fouled the carbon steel pipe walls of the University of Minnesota pipeline, no buildup was observed at any point in the intermittent studies over the course of several years. It is important to know that for some oils successful and permanent lubrication can be achieved in a fouled pipe without further buildup of fouling. This is related to the oil in the core not attaching to fouled oil on the pipe wall. The bitumen froth is well protected against such attachment by a protective layer of clay particles (see § 6) but Zuata readily sticks to itself.

The first studies of self-lubrication of bitumen froth were carried out in 1985 (see Neiman 1986). Tests were conducted in batch with froth generated from an experimental extraction pilot unit. The froth was recirculated in a 50 mm diameter by 47 m long pipeloop test facility. These studies were of short duration, usually 1 hour, 2 hours at most. Relatively fresh froth was used, at varying water volume fraction of 29–37%. In some tests water was added to increase the water fraction to as high as 62%. The froth pipelining temperatures ranged between 45 °C and 95 °C, with most of the tests at 50 °C or 80 °C. These are process temperatures for warm water and hot water extraction techniques, respectively.

Neiman found that the pipeline flow of froth was governed by 'a special type of multi-phase behaviour involving separated water'. A concentration of water was observed to occur near the pipe wall, which effectively formed a lubricating water layer around the central plug of froth. As a result, measured pipeline headlosses were up to two orders of magnitude less than those theoretically predicted by assuming a homogeneous viscous behaviour of the froth. Neiman concluded that 'Pipelining of froth in the Syncrude expansion case may be considered technically and economically feasible'.

Neiman's study did not test the effect of some of the critical issues involved in commercializing the core–annular flow of bitumen froth, such as bitumen fouling, lower temperature effects and flow restart characteristics following flow interruptions. He did not test the full range of the limits of operability and did not explain the mechanisms of self-lubrication of bitumen froth. All these features have been addressed in the studies reported here.

The University of Minnesota studies were also carried out with froth recirculated in a return loop. In fact, this condition is more representative of a long commercial line than a continuous injection of new froth through the short pilot pipelines used in the laboratory studies. We used two different batches of froth. The water volume fraction in these varied between 22% and 40%. Most of the tests were typically eight hours long, others were 48 hours and the longest one was 96 hours. The tests were carried out in the range 35–55 °C, where the temperature level is strongly influenced by frictional heating.

The University of Minnesota studies have suggested that the released water is es-

sential to the development of self-lubrication, mainly due to the presence of kaolonite (clay) particles in a colloidal suspension. They also indicated that there is a minimum velocity below which self-lubrication fails but no such limitation has been found for high velocities. The pilot-scale tests were carried out in a closed loop at Syncrude, Canada. These tests were 2, 24 and 36 hours long, and the temperature ranged between 45 °C and 55 °C.

2. The experiments

2.1. *Minnesota tests*

Froth was recirculated in a 25 mm diameter, 6 m long return loop. A schematic of the test facility is shown in figure 1. Two loops (*main* and *secondary*) are interconnected in this facility. Froth circulates through the main loop, driven by a positive displacement pump (Moyno pump). The flow rate or the speed of the froth in the pipeline is easily determined from the pump's r.p.m. and the pressure discharge. It also can be measured by direct visualization using a high-speed video camera. To prevent oil from sticking to the pressure gauges we mounted a buffer chamber assembly (US patent 5,646,352), which allows only water to get into the chamber and thus prevents oil from sticking to the pressure gauges. The detail of figure 1 shows a device used to visualize and take samples of the circulating froth. It is composed of a removable section and a bypass pipe. The removable section is a glass pipe directly connected to the main test pipeline. The secondary loop provides the main loop with water for cleaning the pipeline; it is also used for start-up of lubricating flow. The start-up of froth in a lubricated mode requires that it be introduced into the pipeloop at a high enough velocity, which may be achieved by injecting froth behind fast moving water. The secondary loop was also used to warm the froth at the inlet of the pipeloop, at every cycle; the inlet of the pipeloop could be heated by circulating hot water through copper tubes rolled inside the supply tank, around the Moyno pump and around part of the pipeline (see figure 1). This setup provided the froth with external heat at the Moyno pump and inlet of the pipeloop. In later experiments, a jacket was mounted around the pipeloop, so warm water could flow around it, which allowed us to control the froth temperature all along the pipeloop.

2.2. *Syncrude tests*

The pilot-scale tests were carried out in a closed loop at Syncrude, Canada. A 0.6 m diameter and 1000 m long pipeline was used. The bitumen froth was recirculated in the loop, driven by a centrifugal pump. Flow rate and pressure drop were measured using an ultrasonic flowmeter and pressure transducers. The data were automatically collected and recorded. Before and after each test, the loop was flushed with tap water. Pressure drop and volume flow rates for water alone (released water from the froth) were also measured for comparison with lubricated froth transport.

3. Results

3.1. *Standard rheological measurements*

The froth viscosity is an ambiguous concept since the release of water under shear lowers the shear stress required to move the froth by orders of magnitude. However, it is still useful to measure it with different kinds of viscometers to characterize froth lubrication under different conditions and to provide upper limits of viscosity and thus a benchmark for computing safety and efficiency factors.

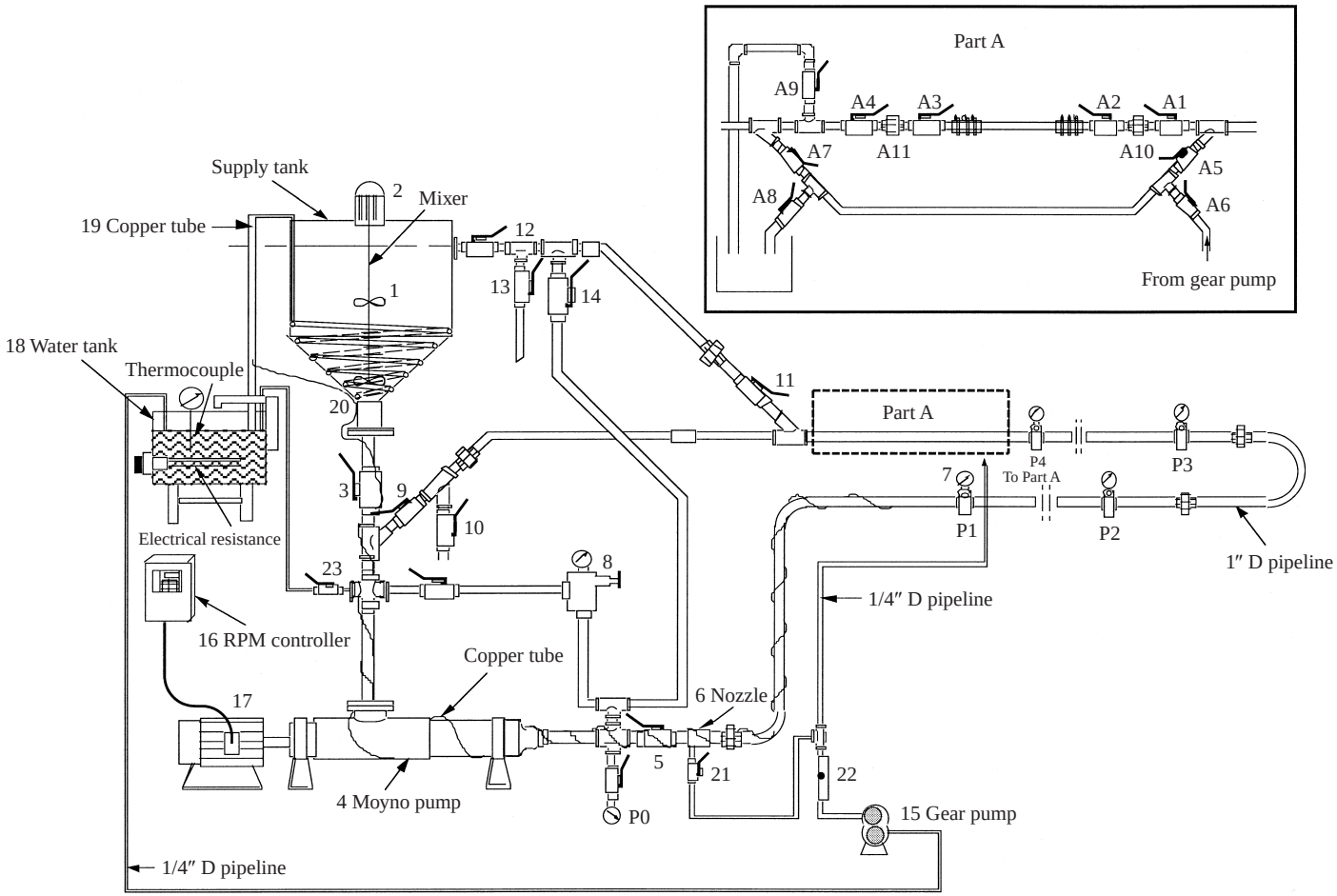

FIGURE 1. Test facility schematic. Two interconnected loops can be easily identified: a main loop, whose principal components are a supply tank, a three stage Moyno pump and a 25 mm diameter; 6 m long pipeline; and a secondary or water loop whose principal components are a water tank, a 6.25 mm pipeline, copper tube and a gear pump. Bitumen froth circulates through the main loop. Pressure taps are labelled as P0, P1, P2, P3, and P4. The distances between them are: 3.86 m (P0-P1), 3.96 m (P1-P2 and P3-P4), and 4.37 m (P2-P3). The sampling system (Part A) is shown in detail.

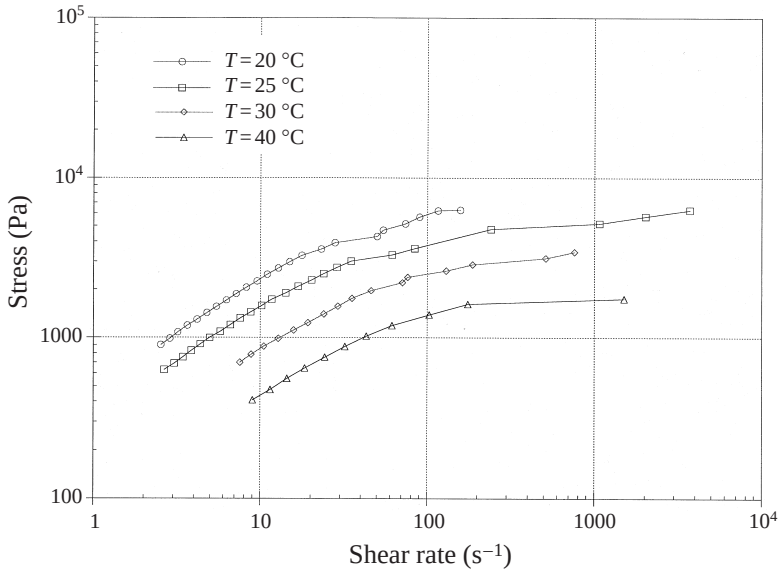

FIGURE 2. Shear stress as a function shear rate at different temperatures for bitumen froth with a water content of 20–22%.

Measurements were carried out on a froth with a water volume fraction Φ of 20–22% in a 22 mm (diameter) parallel plate viscometer (Rheometrics) at temperatures ranging between 20 °C and 40 °C. Figure 2 shows that the slope of the shear stress dramatically changes for shear rates greater than 100 s^{-1} for all the temperatures. The effect is even more dramatic at high temperatures. This levelling of the shear stress vs. shear rate suggests that the froth has entered self-lubrication; the shear stress does not change on increasing the shear rate.

The consequences of self-lubrication for measurements of viscosity are instrument specific. A parallel plate has, in principle, a constant shear rate throughout, but the shear rate varies in capillary tubes, with the greatest shear rates at the wall, promoting water release there.

The released water in the froth is a colloidal dispersion of small clay particles. The density of this water is slightly larger than that of water, $\rho = 1.05\,\mathrm{g\,cm^{-3}}$ at 20 °C. The variation of density with temperature is small and we may take $\rho = 1\,\mathrm{g\,cm^{-3}}$ with only small errors. We measured the viscosity as a function of temperature: it varies from 1.6 cP at 20 °C to 0.8 cP at 50 °C. In our estimates we use the value 1 cP for released water.

3.2. *25 mm diameter pipe tests*

Bitumen froth was continuously recirculated for between 3 and 96 hours. Pressure gradients were measured for velocities between 0.25 $\mathrm{m\,s^{-1}}$ and 2.5 $\mathrm{m\,s^{-1}}$. Some velocities were kept constant for less than 30 min and others up to 48 hours. The temperature T ranged between 35 °C and 55 °C, where the increase of temperature is due frictional heating. The volume fraction Φ of water in the froth ranged between 20% and 40%. Attention was focused on the stability of the greatly reduced pressure gradients, which are associated with water lubrication, over long periods of time, showing that the buildup of fouling does not occur.

In two different tests, we observed large increases and fluctuations in the pressure,

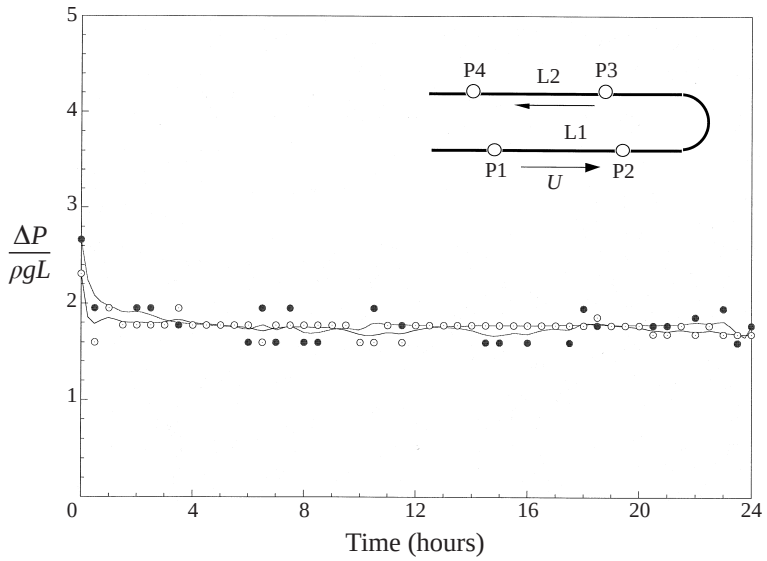

FIGURE 3. Dimensionless pressure gradient $\Delta P/L\rho g$ history between two consecutive pressure taps in the forward (•) and return (○) legs of the pipeline. L1 = L2 = 3.96 m. In this case, $\Phi = 27\%$, $U = 1.5\,\mathrm{m\,s^{-1}}$ and $T = 37\,^{\circ}\mathrm{C}$.

when the velocity was reduced to $0.5\,\mathrm{m\,s^{-1}}$; at this value the lubricating pattern failed and the pipeline was blocked. This failure appears to be associated with capillary instabilities in which slugs of bitumen froth form from the continuous core. The existence of a lower limit of speed for the successful operation of core–annular flow is well known for the pipelining of heavy crudes and is of obvious interest for the self-lubrication of bitumen froth. In large diameter pipes, gravity is more important than capillarity and the failure at low speed will give rise to stratification of heavy and light components. We were able to start the stopped line by slow injection of water with the Moyno pump.

The longest test was for 96 hours. Pressure gradients were measured for superficial velocities between 1.0 and $1.75\,\mathrm{m\,s^{-1}}$. The corresponding dimensionless pressure gradients $\Delta P/L\rho g$ ranged between 1.5 and 2.4. No buildup of fouling was observed and the pressure gradients did not increase at any velocity, as illustrated in figure 3. The test started in a pipeline fouled from previous tests; flushing with tap water did not totally remove the oil on the wall. These features show that the buildup of pressure, which would occur if there was an accumulation of fouling, does not occur. Mean values of the pressure were calculated for each tap at each velocity. A decrease of the length of the waves (see figure 12) on the bitumen froth was observed at high speeds and it seemed that less free water was present. The average temperature of the froth increased because of the frictional heating to around $T = 42\,^{\circ}\mathrm{C}$. It is possible that some free water is reabsorbed into the froth at high temperatures as has been suggested by Neiman (1986), who found that heating and water-dilution affect the lubricating layer.

The dimensionless pressure gradients in all tests (available upon request) are low and more or less independent of the water fraction for $22\% \leqslant \Phi \leqslant 40\%$. The scatter of data was least for $\Phi = 22\%$ and greatest for $\Phi = 40\%$.

We also found that providing the froth with external heat (at the Moyno pump and entrance of the loop) does not improve the already excellent lubricating pattern

U ($m\,s^{-1}$)	Released water (water/core)	Core (water/oil)	Total (water/oil)
1.5	5/95	23/72.2	28/72.2
1.75	2.7/96.3	25/71.4	27.7/71.4
2.0	7/93	21.4/71.6	27.4/71.6

TABLE 1. Released water and volume fraction of water in the core in a lubricated transport mode. The original froth samples were 27% water.

in our 25 mm diameter pipe. Heating of bitumen froth can promote the reabsorption of the released water into the core, but it also lowers the bitumen viscosity; flow resistance is then determined by competing effects of water depletion and viscosity reduction.

In another test the temperature was not controlled. Bitumen froth was recirculated for one hour using a Teel Centrifugal Pump (model J.L). We changed the velocity U in four steps, from $4.0\,m\,s^{-1}$ to $0.84\,m\,s^{-1}$. The initial values of temperature and velocity were $T = 30\,^{\circ}C$ and $U \approx 1.5\,m\,s^{-1}$; it took 30 minutes to reach a velocity of $4.0\,m\,s^{-1}$ and a temperature of $T = 61\,^{\circ}C$. The dramatic rise in temperature is due to frictional heating at high froth velocity. Tiger waves (figure 12) were observed at all temperatures.

Froth samples were taken for three different velocities (1.5, 1.75 and $2.0\,m\,s^{-1}$) in two separate tests. By carefully pouring the released water into another container, froth and free water were separated and weighed. The water content of the remaining froth was measured by distillation. The water content of the original froth (water-to-oil ratio before being pumped) was also measured. The results are reported in table 1. In the case of the recirculated froth, this ratio was reconstructed from a mass balance: the mass of water is the sum of released water and water in the core; the mass of oil is the mass of froth minus the water in the core. The water/oil ratio before and after the froth was recirculated match within the expected error.

3.3. *Pilot-scale tests*

Three pilot-scale tests were carried out in a 0.6 m diameter, 1000 m long pipeloop at Syncrude, Canada. The pressure and flow readings were monitored. In the first test, bitumen froth was recirculated for 24 hours. There was no increase of the pressure drop and other bitumen fouling related problems. However, for a fixed pressure drop across the loop (centrifugal pumps provide a constant pressure when the r.p.m. is fixed), the froth temperature and velocity decreased as the night approached. The temperature changed from 47 °C to 43 °C and the velocity from 1.10–$1.14\,m\,s^{-1}$ to $0.90\,m\,s^{-1}$. In the next test core–annular flow was readily and predictably established at a temperature of about 55 °C. First, the froth velocity was maintained at about $0.9\,m\,s^{-1}$ for 2 hours of steady operation. Then the pump drive speed was raised and lowered in steps. At each speed, pressure and flow readings were monitored for about 10 min. There was no hysteresis observed either in the velocity or pressure. The average of the two sets of data at a given speed was used for further analysis. Following the successful completion of the flow variability tests, flow interruption and restarting tests were carried out. However, the details will not be discussed here. In the last test, froth was continuously pumped for 36 hours. During this test, the froth temperature oscillated between 42 °C and 47 °C. The temperature steadily decreased

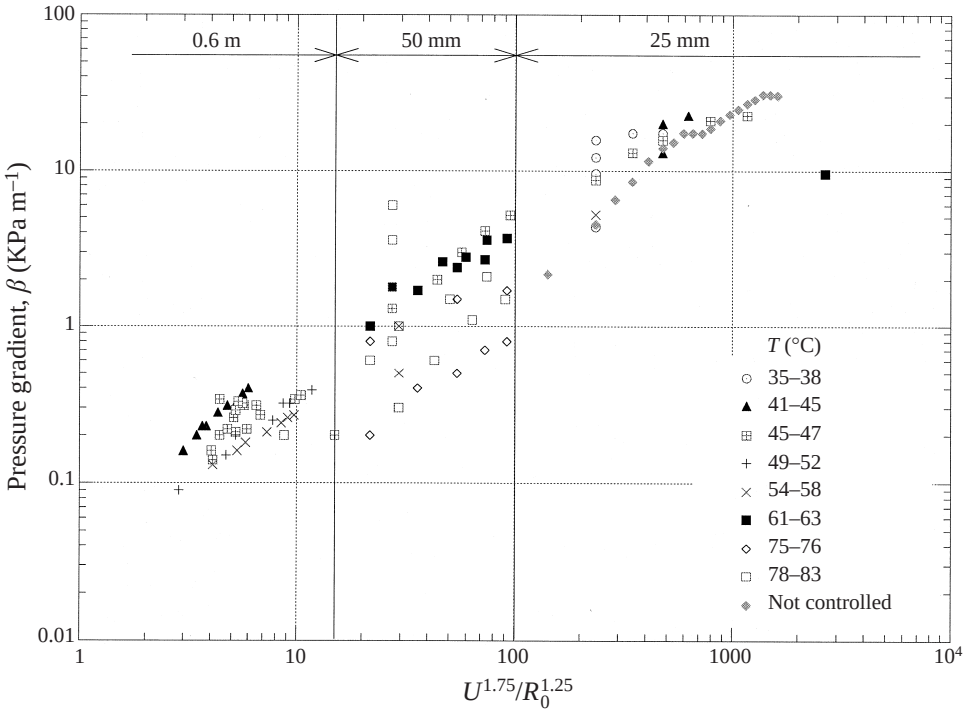

FIGURE 4. All available data for pressure gradient of bitumen froth β [KPa m^{-1}] as a function of the Blasius ratio, parametrized by temperature. Left: 0.6 m diameter pipeline; middle: 50 mm diameter pipeline (Neimans' data); and right: 25 mm diameter pipeline.

during the night (from 8 pm to 8 am) and gradually increased during the day (from 8 am to 8 pm) reaching its maximum in the early afternoon (at about 2 pm). The froth velocity oscillated in the same manner, increasing with temperature. This suggests that the flow resistance was mainly determined by viscosity reduction.

4. Analysis of data

4.1. *Hydrodynamic behaviour*

Figure 4 presents the measured pressure gradient of bitumen froth β[KPa m^{-1}] as a function of the Blasius ratio (the ratio of the $\frac{7}{4}$th power of the velocity to the $\frac{5}{4}$th power of the pipe radius), parametrized by temperature. Three regions can be easily identified, corresponding to the data collected in the 0.6 m, 50 mm and 25 mm pipelines. All the available data are shown in figure 4. The 50 mm diameter pipeline data of Neiman (1986) are greatly scattered and will be mostly ignored in our analysis.

Data in a high temperature (49–58 °C) range and a low temperature (38–47 °C) range collapse into two curves parallel to the Blasius' formula for turbulent pipeflow (for Reynolds numbers below 3×10^6). These curves are shown in figure 5. The parameters defining these curves are presented in table 2 and were determined by the following considerations.

A force balance per unit length gives a relationship between the pressure drop β

Temperature range (°C)	K	Corresponding k (approx.)
38–47	40.5×10^{-3}	6
49–58	28.1×10^{-3}	3

TABLE 2. Fitting constant K for two temperature ranges, using equation (4.5).

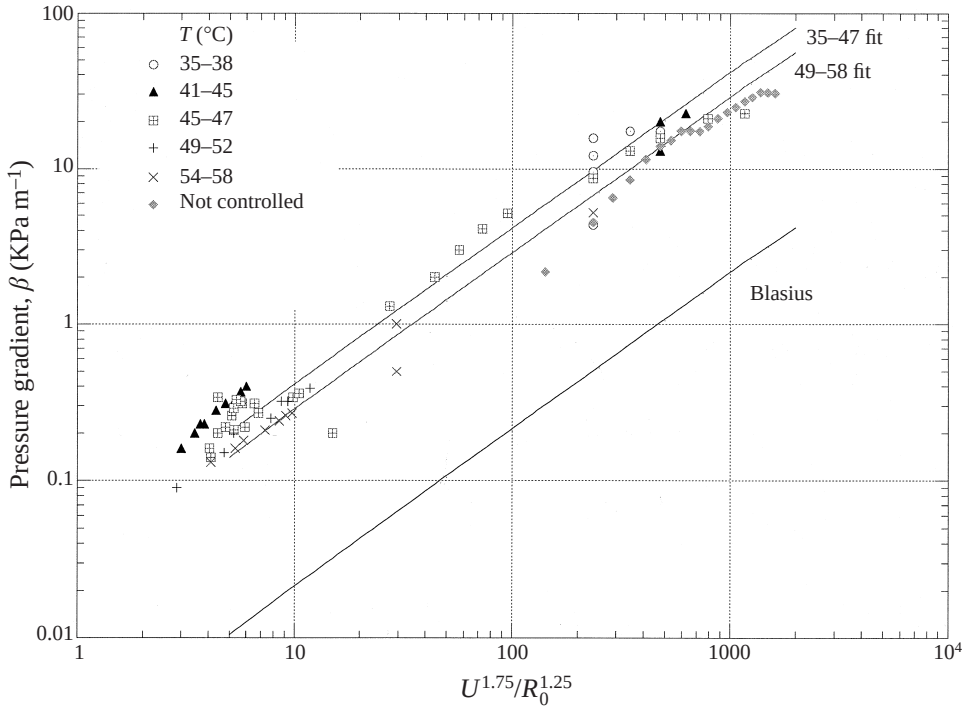

FIGURE 5. Curve fits parallel to the Blasius correlation for turbulent pipeflow (bottom line), for two temperature ranges: 35–47 °C (top) and 49–58 °C (middle) presented in figure 4. Most of the 50 mm diameter pipeline data were ignored in these fits, due to their high scatter.

and the shear stress τ_w on the pipe walls:

$$\tau_w = \frac{\beta R_0}{2} \tag{4.1}$$

where R_0 is the pipe radius. But the shear stress τ_w may be expressed as function of a friction factor λ defined as follows:

$$\lambda = \frac{8\tau_w}{\rho U^2}. \tag{4.2}$$

We now introduce an empirical correlation (based on the Blasius' formula):

$$\lambda = \frac{k}{Re^{1/4}} \tag{4.3}$$

where k is an unknown constant ($k = 0.316$ for water alone) and Re is a Reynolds

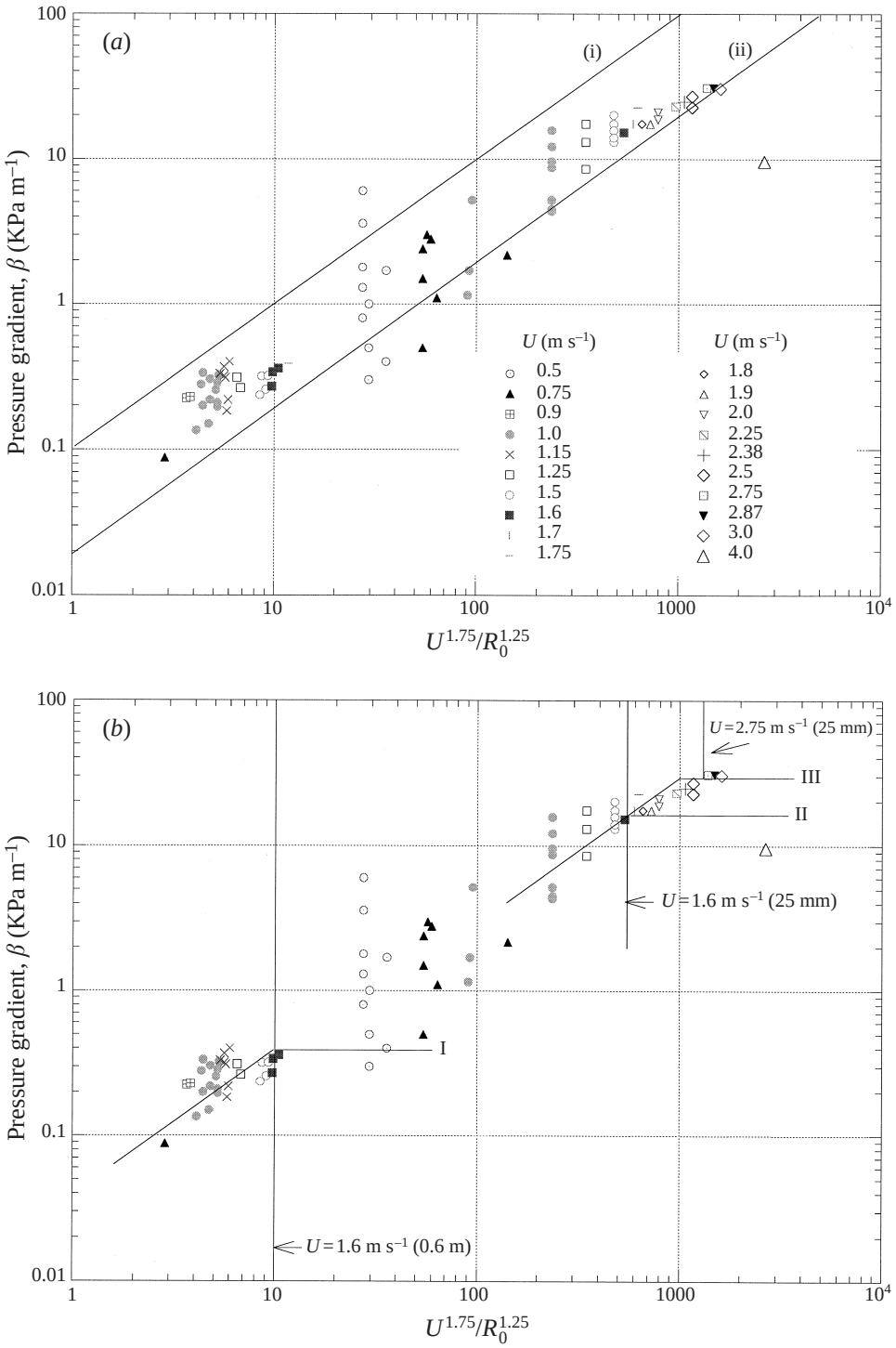

FIGURE 6. For caption see facing page.

number defined as

$$Re = \frac{2R_0 U}{v} \tag{4.4}$$

where v is the kinematic viscosity of water. The Blasius formula (4.3) holds for $2100 < Re < 10^5$; it was developed from the $\frac{1}{7}$th power law velocity distribution.

Combining equations (4.1) to (4.4) we can obtain an expression for the pressure gradient β [KPa m^{-1}], in terms of the $\frac{7}{4}$th power of the velocity U [m s^{-1}] to the $\frac{5}{4}$th power of the pipe radius R_0[m], namely

$$\beta = K \frac{U^{7/4}}{R_0^{5/4}}. \tag{4.5}$$

K was determined from a best fit for given values of U and R_0 and measured β; K determines the constant k previously defined.

Table 2 shows that the pressure gradient β, hence K and k (≈ 6) for froth, is 10 to 20 times larger than the Blasius values for water alone ($k = 0.316$); the increase in the pressure gradient over and above the Blasius value observed in figure 5 is of the order of 10 to 20 and it is independent of velocity or pipe size.

Figure 6 presents again all the available data, but now parametrized by velocity rather than temperature. In figure 6(*a*), curves (i) and (ii) enclose most of the data, if the scatter in the 50 mm diameter pipeline data region is ignored. They are respectively our subjective estimate of the most pessimistic and least pessimistic predictions for β based on Blasius' formula. Another point of view is given by figure 6(*b*). There, curves I and II and III (also determined by a subjective estimate from the visual inspection of the data) predict the pressure gradient based on a velocity criterion, for the 0.6 m and 25 mm pipes. These curves are parallel to the Blasius' formula and most of the points are located between curves (i) and (ii) (see figure 6*a*). The existence of critical values for a more complete lubrication is suggested by the data. At these values the pressure gradient reaches a plateau and does not increase as the velocity is increased. This kind of lubrication can be called 'something for nothing'; it is possibly a robust phenomenon associated with frictional heating of froth (see figure 7).

Figure 7 shows the pressure gradient vs. the Blasius parameter $U^{7/4}/R_0^{5/4}$ together with the froth temperature, in the case in which the wall temperature is not controlled; the temperature values are marked on the plot. The points on figure 7 are included in the data shown in figures 4, 5 and 6; they follow the Blasius law up to the first critical value $U = 1.6\,\mathrm{m\,s^{-1}}$ after which they exhibit the flattening transition already discussed. At a value of $U \approx 2.0\,\mathrm{m\,s^{-1}}$ the curve begins to rise again to a second flattening transition at $U = 2.75\,\mathrm{m\,s^{-1}}$. The temperature increases monotonically with flow speed and the temperature rise is substantial.

Figure 8 shows the same data plotted as temperature vs. velocity. The temperature rise is nearly proportional to U^2; this is consistent with frictional heating generated

---

FIGURE 6. Pressure gradient of bitumen froth β [KPa m^{-1}] as a function of the Blasius ratio, parametrized by velocity. Left: 0.6 m diameter pipeline; middle: 50 mm diameter pipeline (Neimans' data); and right: 25 mm diameter pipeline. (*a*) All available data, enclosed by the most pessimistic (i) and least pessimistic (ii) predictions for β based on Blasius' formula, and ignoring the scatter in the 50 mm diameter pipeline data region. These two curves were chosen arbitrarily from inspection of the data. (*b*) I and II and III are predicted pressure gradients β, based on a velocity criterion, for the 0.6 m diameter pipeline data and 25 mm diameter pipeline data. Here the critical velocity is approximately $U_c = 1.6\,\mathrm{m\,s^{-1}}$ for curves I and II and $U_c = 2.75\,\mathrm{m\,s^{-1}}$ for curves III.

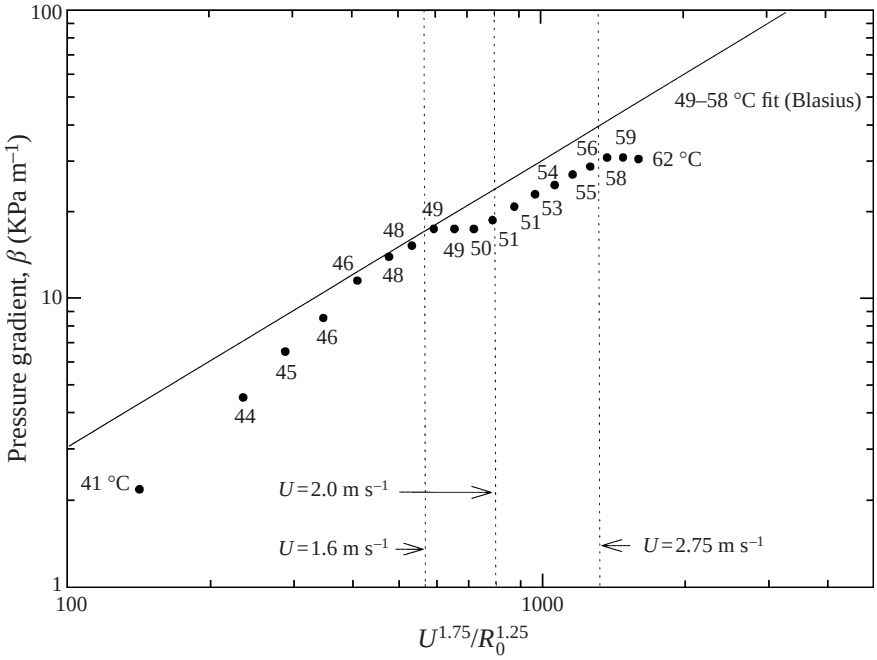

FIGURE 7. Pressure gradient vs. Blasius parameter in the 25 mm diameter pipe. The temperature of the room was 26 °C and the froth temperature (the numbers labelling the data points) was not controlled; the increase in temperature is due to frictional heating as shown in figure 8.

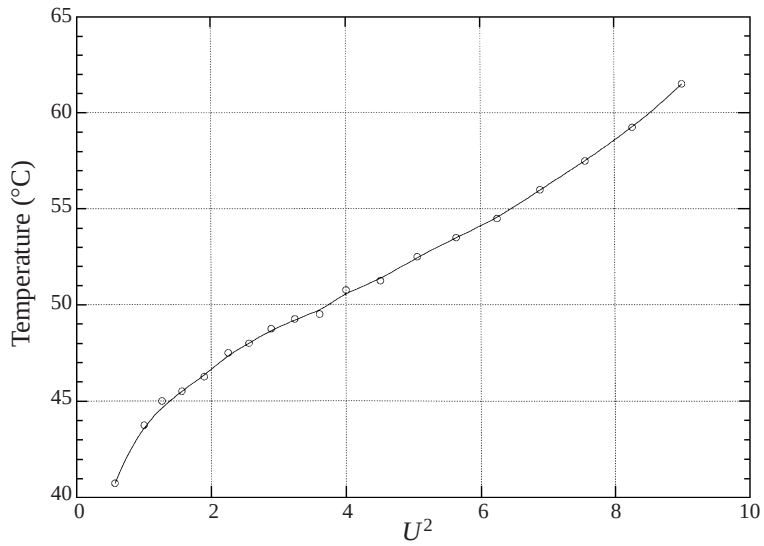

FIGURE 8. Temperature vs. the square of the flow speed for conditions specified in figure 7; the rise in temperature is approximately linear suggesting frictional heating.

by a heat source of magnitude $\overline{\mu}\left(\mathrm{d}\overline{u}/\mathrm{d}y\right)^2$ where $\overline{u}$ is an effective viscosity and $\mathrm{d}\overline{u}/\mathrm{d}y$ an effective shear rate in a layer of sheared froth near the wall. The data should be useful for modelling the effects of frictional heating.

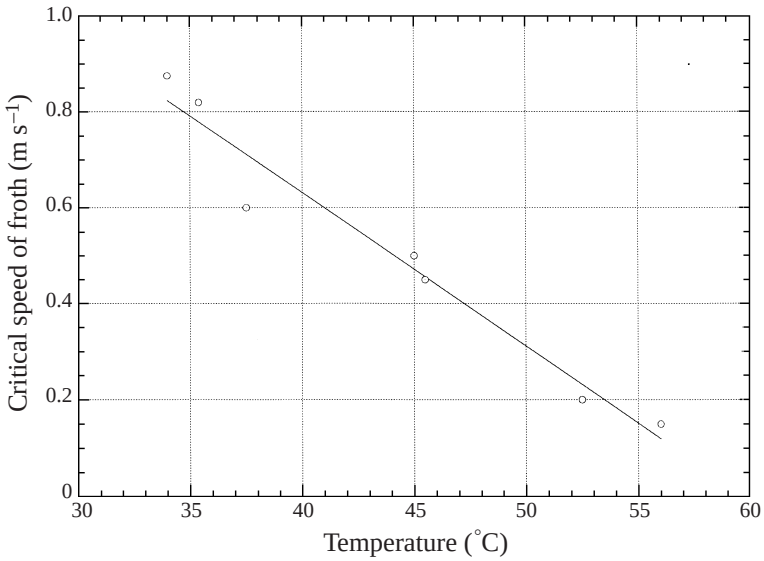

FIGURE 9. Froth velocity at which self-lubrication is lost as a function of the froth temperature. Self-lubrication is more persistent at high temperatures.

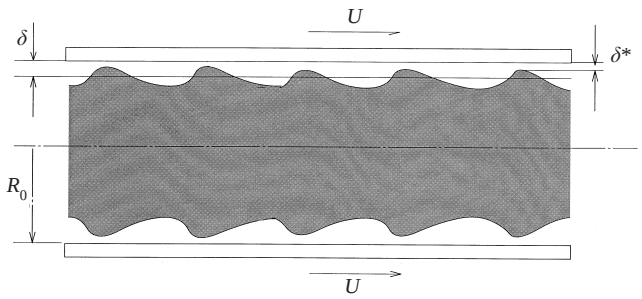

FIGURE 10. Released water layer thickness δ for self-lubricated froth flow. R_0 is the pipe radius and $\delta/R_0 \ll 1$. The frame of reference has been changed: the bitumen froth core is fixed and the pipe wall moves with the measured average velocity of the froth U.

We have already noted that there is a critical value for the start of self-lubrication, which we have not found yet. There is also a critical value for the loss of self-lubrication, which we believe is smaller than the start critical value. We also believe that it depends on the froth temperature which changes with speed, due to frictional heating. Hence, in principle, we should find one loss value by reducing the pressure gradient in steps after allowing the temperature to equilibrate in each step. To see how this critical value varies with the temperature we circulated warm water all around the pipeloop through the jacket mentioned in § 2.1. The result of this study is shown in figure 9. Lubrication can be maintained at smaller speeds when the froth temperature is larger, suggesting that lubrication might be difficult to maintain at very low temperatures. Fortunately the froth temperature is naturally substantially raised in working pipelines by frictional heating.

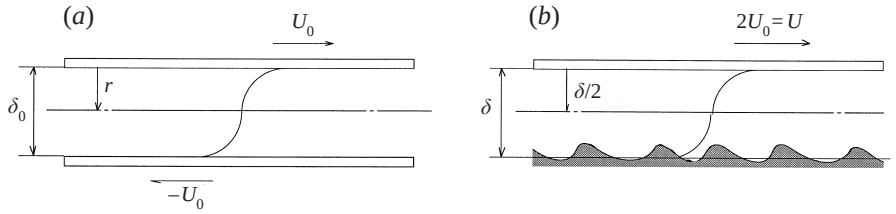

FIGURE 11. Turbulent Couette flow from Reichardt (1956). (*a*) Two parallel plates, separated by a distance δ_0, are moved in opposite directions with a velocity U_0. The distance from the wall to the centre of the channel is denoted by r. (*b*) The frame of reference has been changed. Now the lower wall is fixed and represents the bitumen froth core, and the upper wall represents the pipe wall, moving at a velocity $U = 2U_0$. Here δ denotes the effective mean gap size.

4.2. *Prediction of the released water layer thickness*

It is possible to estimate the thickness of the water layer, as well as the associated water volume fraction, when bitumen froth is flowing with an average velocity U in a pipe of radius R_0. Figure 10 shows a cartoon of the released water flow between the wavy bitumen froth core and the pipe wall. We can define an effective mean gap size δ, which is the distance between the wall and a perfectly smooth bitumen froth core. We can also change the frame of reference: fix the core and let the wall move with the measured average velocity U of the froth.

Let X be the mass fraction of free water with mean depth δ for a given flow velocity U and a pipe radius R_0. We suppose that the mass fraction is equal to the volume fraction and the ratio of the volume of water in an annulus of thickness δ to the total volume of water is the same as the ratio of the area of the annulus to the total area. Hence,

$$X = \frac{R_0^2 - (R_0 - \delta)^2}{R_0^2} \approx \frac{2\delta}{R_0} \tag{4.6}$$

when $\delta \ll R_0$.

The core flow of the bitumen cannot be turbulent because the viscosity of bitumen is so large. The water flow in the thin annulus is turbulent; strong turbulence was observed in the viewing window and our data fits curves parallel to the Blasius curve for turbulent pipeflow. An attractive way of predicting the water layer thickness δ is given by Reichardt's (1956) model of turbulent Couette flow, which is a version of the universal law of the wall. Figure 11(*a*) illustrates this model: two parallel plates, separated by a distance δ_0, are moved in opposite directions with a velocity U_0. The fluid inside is sheared giving rise to an 'S'-shaped velocity profile, which is described by

$$\frac{U_0}{u^*} = 2.5 \ln (2\eta_r) + 5.5. \tag{4.7}$$

Here η_r is a dimensionless length, defined as follows:

$$\eta_r = \frac{ru^*}{\nu} \tag{4.8}$$

where $r = \delta_0/2$ is the distance from the wall to the centre of the channel, u^* is the friction velocity and ν is the kinematic viscosity of the water.

The friction velocity u^* is

$$u^* = (\tau_w/\rho)^{1/2} \tag{4.9}$$

U ($\mathrm{m\,s^{-1}}$)	Released water layer thickness (mm)		Released water mass fraction (%)	
	Measured (δ)	Calculated (δ_k)	Measured (X)	Calculated (X_k)
1.5	0.3	0.26	4.7	4.2
1.75	0.17	0.36	2.7	5.7
2.0	0.44	0.80	6.9	13

TABLE 3. Measured and calculated released water layer thickness δ and volume fraction for self-lubricated froth flow in a 25 mm diameter pipe.

where ρ is the water viscosity and τ_w is the shear stress on the wall, given by equation (4.1).

If we now change the frame of reference and let the wall move with a velocity $U = 2U_0$ and let $r = \delta/2$, as shown in figure 11(*b*), an expression for the released water layer thickness δ may be obtained from equation (4.6), as a function of U and u^*:

$$\delta = \frac{v}{u^*}\exp\left(\frac{0.5\,U/u^* - 5.5}{2.5}\right). \tag{4.10}$$

Equation (4.10) predicts values of δ of order 10^{-3} mm for the 25 mm and 0.6 m diameter pipelines. These values do not agree with the values obtained from the mass balances carried out in the 25 mm diameter pipeline tests, which are listed on table 3. We presume that this small gap is between the pipe wall and the crests of the waves, indicated as δ^* in figure 10. However we are interested in predicting the mean gap size δ, which is much larger.

Since we know that our data fits Blasius' formula with a friction factor ($k/0.316$) times greater than the one given by equation (4.2), or

$$\lambda_k = \frac{k}{0.316}\lambda_{\mathrm{Blasius}} \tag{4.11}$$

we can define a pseudo friction velocity as follows:

$$u_k^* = \left(\left(\frac{0.316}{k}\right)\frac{\tau_w}{\rho}\right)^{1/2}, \tag{4.12}$$

where the factor ($0.316/k$) alters the measured value of the shear stress τ_w (obtained from the pressure drop). Now, if we let $u^* = u_k^*$, equation (4.10) becomes

$$\delta_k = \frac{v}{u_k^*}\exp\left(\frac{0.5\,U/u_k^* - 5.5}{2.5}\right). \tag{4.13}$$

We used equations (4.13) and (4.6) with $k/0.316 = 20$, to calculate the values of the water layer thickness δ_k and the corresponding mass fractions X_k. These values are listed in table 3, where they are compared to the values obtained from the mass balances; given the mass (volume) water fraction X, the water layer thickness δ may be computed using equation (4.7). The agreement in the order of magnitudes is obvious. Effects of temperature, which are not considered in this model, may be the source of the discrepancy between the measured and calculated values of δ. Frictional heating is very important at high velocities and an increase in temperature may promote reabsorption of some of the released water. More research is required

U ($m\,s^{-1}$)	Released water layer thickness δ (mm)	Released water mass fraction X (%)
1.0–1.75	1–7	1–5

TABLE 4. Predicted released water layer thickness δ_k and volume fraction for self-lubricated froth flow in a 0.6 m diameter pipe.

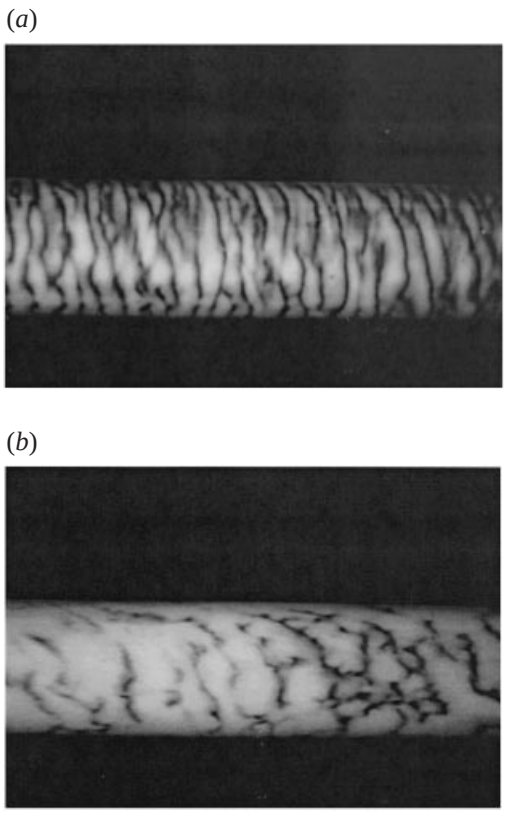

FIGURE 12. 'Tiger' waves for $U = 1.0\,m\,s^{-1}$ (*a*) and $U = 1.5\,m\,s^{-1}$ (*b*) in a 1″(25 mm) diameter pipe. They are like the waves that develop in core-annular flows and can be seen where the free milky water layer is thin. The released water is a dispersion of small clay particles water.

to validate and improve this model; for the moment, the predictions of the released water fraction for the 0.6 m diameter pipe data are satisfactory and consistent with the water fractions calculated for the 25 mm diameter pipe data (see table 4).

5. Mechanism of self-lubrication of bitumen froth

Bitumen froth is a very special kind of multi-phase material. It combines properties of an oil continuous phase in which water is the dispersed phase with properties of a water continuous phase, like oil-in-water emulsions. In usual oil–water mixtures, dispersions of 22–40% water in oil are very stable and very viscous with viscosities even higher than the oil alone.

The dispersion of 22% water in bitumen would be robustly stable as an ordinary two-phase mixture. A monosized dispersion of 78% bitumen drops in water is not possible because such a concentrated dispersion could not be packed. A 22% water froth in a pail looks like a pure bitumen, since no free water can be seen. It is extremely viscous to low shearing, but is unstable to faster shearing which causes water droplets to coalesce and form a free lubricating layer of free water. In fact, tests indicate a tendency for droplets of water to coalesce even under static conditions.

The unusual properties of bitumen froth with respect to the coalescence of water droplets leading to self-lubrication are due to released water being a dispersion of small clay particles in the water, giving it a grey colour which can be called milky. The milky appearance is persistent because the small particles are of colloidal size $O(\mu)$, held in suspension by Brownian motions. When water is released at the wall in a pipe flow, it is opaque except where there are 'tiger' waves, which are like the waves which develop in core–annular flows, where the released water layer is thin at the crests (see figure 12). The free milky water is roughly 20–30% by weight of the original water in the sample, so that quite a lot of coalescence has occurred. (The weight fraction of the free water relative to the weight of the mixture defining the froth core is just a few percent.)

The clay water inhibits the coalescence of bitumen froth and promotes its own coalescence through a mechanism like powdering dough: dough is sticky, but when you put flour on it, the dough is protected against sticking by a layer of powder. The clay in the released water is just like powder: it sticks to the bitumen froth and prevents it from coalescing. Zuata crude is much more sticky than bitumen froth and it sticks strongly to glass and plastic bottles filled with water, but not when filled with released clay water; this is very remarkable and totally unexpected.

The action of the clay particles is very much like the action of surfactants which are used to stabilize emulsions. Yan & Masliyah (1994) have investigated the absorption and desorption of clay particles at an oil–water interface. They note that it is generally accepted that hydrophilic particles (clay) stabilize oil-in-water emulsions while hydrophobic solids stabilize water-in-oil emulsions. The fine solids absorbed on the droplet tend to act as a barrier, protecting the oil droplets from coalescing with one another. Yan & Masliyah studied the effect of kaolinite clay particles on stabilization of oil-in-water emulsions using a multilayer absorption model. As in the theory of absorbed surfactants, absorption isotherms relating the bulk concentration to the surface excess are important. They note that "...To obtain a stable solids-stabilized oil-in-water emulsion, it is necessary for the droplets to be covered by at least a complete monolayer of particles." This is like the critical micelle concentration in which the interface is fully saturated and cannot absorb more surfactant. Obviously, enough clay must be in the water to fully cover the drop surface, to powder the dough.

The released water readily fingers through the froth; the channels in the froth cannot close off because the protective film of clay particles prevents the froth from sticking to itself. This is the mechanism for self-lubrication of bitumen froth with released water. The droplets are strongly stretched by shear forces at the wall. The froth which is protected by absorbed clay particles is also stretched, but it cannot coalesce or pinch off the water streamers because of the protective particle layer. This promotes the coalescence of the extending droplets of released water into sheets of lubricating water. The annulus of lubricating water can work perfectly well between 'powdered' froth layers since these protected layers will not coalesce when touching. The bitumen froth may therefore foul the pipe wall and still not interfere with the smooth lubrication of the froth core.

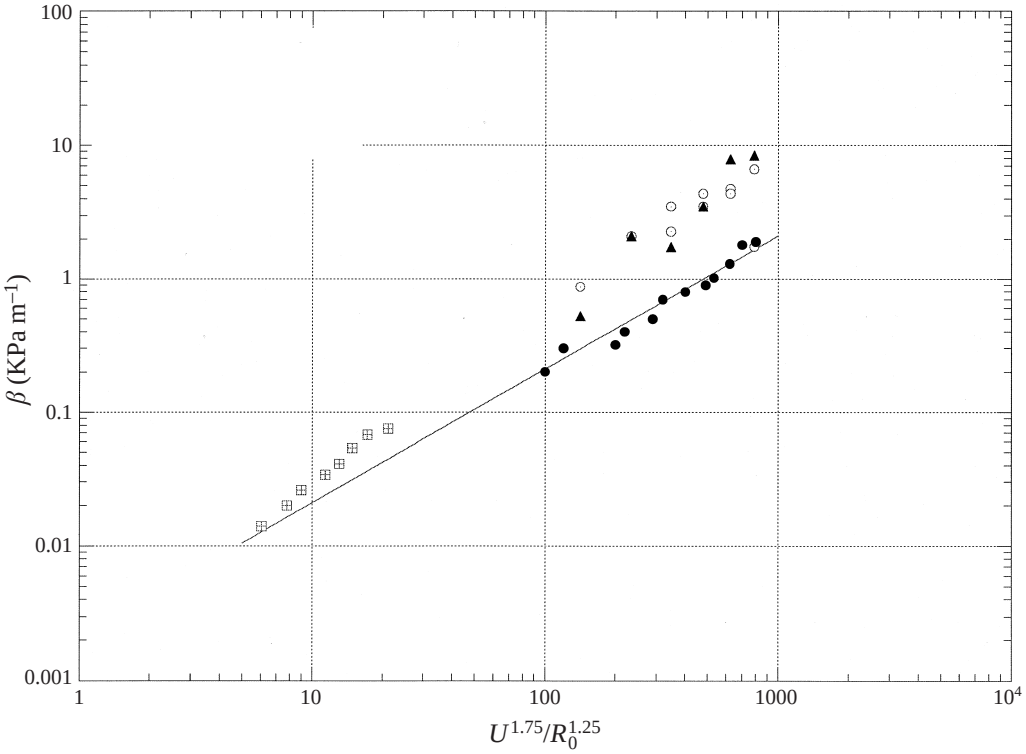

FIGURE 13. Pressure gradient β [KPa m^{-1}] of tap and/or released (clay) water : ○, tap water and ▲, released water for the 25 mm pipeline before cleaning; ●, tap water for the 25 mm pipeline after cleaning; ⊞, released water for the 0.6 m pipeline. The bottom line is the Blasius correlation for pipe which when expressed in terms of the friction factor λ is $\lambda = 0.316\,Re^{-1/4}$.

An idea suggested by self-lubrication of froth in clay water is that fouling of pipe walls by heavy oils may be relieved by adding hydrophilic solids of colloidal size to the water in a concentration above that necessary for saturation of the oil–water interface. This "powdering of the dough" works for clay particles.

To establish this idea we sheared some bitumen froth between two 75 mm diameter glass parallel plates. One plate was rotating and the other was stationary. We found that water was released inside, fracturing the bitumen. The internal sheet of water was sandwiched between two layers of bitumen, which stuck strongly to the glass plates. The bitumen on the moving plate rotated with the plate as a solid body. The froth fractured internally as a cohesive fracture and not as an adhesive fracture at the glass plates. Some of the water in the sandwich centrifuged to edges. The experiments proved that you can lubricate froth from froth with clay water.

6. Creation and removal of fouling

The experiments in Minnesota and Syncrude's pilot showed that the pipeline walls were fouled with bitumen froth but a buildup of fouling was never observed. We may postulate that the pipe is continuously fouled and cleaned by running clay water without depletion or accumulation.

The pressure drop for self-lubrication of froth was compared with the measured pressure drop for water alone in the 0.6 m pipe and it was 10 to 20 times larger. To

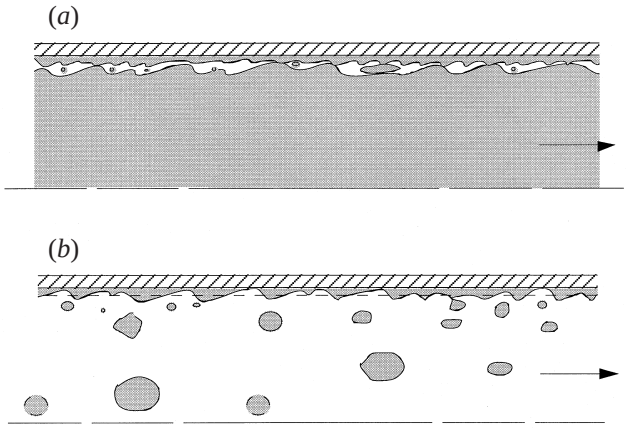

FIGURE 14. Cartoon of standing waves of fouled oil with drops being sheared off the crests: (*a*) tiger waves of the core in self-lubrication of froth, (*b*) water alone pipelining.

explain this discrepancy, we compared measured values with water alone in pipes at both test centres with the Blasius' formula (4.4) and (4.5) which ought to apply. The Minnesota data were nearly 10 times larger than the theoretical value; the Syncrude pilot data were also higher but much less so (figure 13). The explanation for this is in the degree of fouling. We found that the pressure gradient in water flow in the 25 mm pipeline at Minnesota could be reduced nearly to the Blasius value by running clay water until oil drops no longer appear in the viewing window. This shows that a fouled pipe can be thoroughly cleaned by running water; pigging is never required. However, we must emphasize that cleaning up a fouled pipeline is not necessary, because fouling and cleaning are in steady state when froth is pipelined.

A pressure gradient price must be paid to wash oil off a fouled wall. Waves must develop on the parts of the wall fouled by oil. These waves probably propagate very slowly, because the fouling layer is very viscous and very thin. Apparently it is even possible that basically standing waves are on the wall and the crests of these waves are torn away to form the oil blobs and drops which appear in the viewing window. A cartoon to visualize this scenario is shown in figure 14. This explanation does not clarify why the observed increase in the pressure gradient is independent of velocity or pipe diameter.

7. Critical conditions for self-lubrication

The results of the 1985–1986 experiments of Neiman and the 1996 experiments at the University of Minnesota indicate that a lubricating layer of water will not form unless the flow speed is large enough. The Neiman experiments in 50 mm pipes do not mention this point explicitly but data for self-lubrication are given only for flow velocities greater than a critical value of the order of $0.3\,\mathrm{m\,s^{-1}}$. The University of Minnesota experiments addressed this point explicitly and they showed that self-lubrication was lost when the flow velocity was reduced below 0.5–$0.7\,\mathrm{m\,s^{-1}}$.

The critical criterion could possibly be expressed by a critical shear stress for water release which depends on the composition and temperature of the froth. If this stress is exceeded, water will be released and the maximum stress in the froth is where it is most sheared, at the water–froth interface. The shear stress is continuous across the interface and in the water it scales with the shear rate. A similar self-lubrication

of water in oil emulsions (5% to 60% water by weight) at a certain shear rate for a certain period of time is found in tests by Kruka (1977) using 10% water in three different Midway-Sunset crudes flowing in a 25 mm pipe.

Experiments have established that there is a critical speed for self-lubrication; below this speed the pressure gradient required is very high and depends on the froth rather than water viscosity. The critical speed may be related to a critical shear stress, but more research is necessary.

8. Start-up and restart of self-lubrication

The bitumen froth first sticks to the wall where it is stretched in the direction of the flow. Spherical drops of water stretch into elongated fingers of water which coalesce; the bitumen does not close off the water streamers because it is protected from sticking to itself by a layer of adsorbed clay. The streamers coalesce into water sheets which lubricate the flow. In fact water streamers which percolate through the froth in regions of high shear provide good lubrication. The shear required to produce percolated strings of coalesced water drops which ultimately form sheets of lubricating water penetrates only partly in the froth. The factors that control the penetration depth have not yet been identified.

High shear rates at the wall are required for self-lubrication. Such shear rates are easily obtained; by injecting the froth behind fast moving water we take advantage of flow development. Even a low-speed fully developed flow can have a high rate of shear at the wall when it is developing. Water release and formation of tiger waves are characteristic of self-lubrication and appear almost immediately after the froth is injected at high speeds behind the turbulent water flow. Pure water or released water can be used for start-up but the velocity of the water and the froth must be above critical. In a field application one would start the froth behind a high-velocity water flow and the water would be automatically expelled from the pipe.

Restarting a pipe after shutdown is difficult because the stopped line is full of static froth which expels lubricating water over time and it becomes harder to restart the flow in the lubricated mode with low pressure gradients. It is necessary to raise the froth speed to a value high enough to generate a shear rate large enough to produce water release and coalescence. The University of Minnesota experiments suggested that it would not be possible to raise the shear rate to a high enough value to produce water release at acceptable pressure gradients without first washing out some froth by straight water injection. In the most extreme case all the froth would need to be expelled and the restart begun as a straight start up, behind fast moving water but this case in unlikely.

Restart after expelling froth is always possible, and since fouled pipes can be cleaned by water flushing, expensive pigging operations will never be required.

9. Concluding remarks

Bitumen froth self-lubricates; even a fouled pipeline may be run without any buildup of fouling or pressure gradient penalty. The mechanism of self-lubrication depends on the froth weakness and clay covering of bitumen which allows water to coalesce and keeps bitumen from sticking to itself. The fouled oil on the pipe wall acts like a protective coating on which further fouling is inhibited by a clay covering. A fouled pipeline may be cleaned by running clay water. There is a critical speed for froth lubrication which may be related to a critical stress. The pressure gradient for

self-lubricated froth flow follows the Blasius correlation, but with a friction factor 10 to 20 times higher. A second critical speed may be identified; after this the flow rate increases greatly for very small increases in the pressure gradient, but a mechanism for this 'super lubrication' is not known. The flow in the water annulus is turbulent, but the flow in the bitumen must be laminar. An *ad hoc* model giving the thickness of the lubricating layer of the clay water consistent with the Blasius law was proposed and shown to be in order of magnitude agreement with hold up measurements.

A whole range of theoretical questions relating to self-lubrication of bitumen froth have been posed but not answered here. These include questions about the critical velocity for start up and for the loss of lubrication, the mechanisms responsible for loss of lubrication, the nature of water release under shear and temperature changes and the effects and analysis of frictional heating. It is probable that the answers to many of these questions are nearly the same as those previously given by us for lubricated rather than self-lubricated lines; the chief difference between the two is the colloidal clay which is necessary for self-lubrication but prevents us from seeing as clearly as we can when water without clay is added. Some tentative remarks addressing these questions may be useful. First we note that bitumen froth which has 30% or 40% water is nearly density matched with clay water, but the mismatch causes the froth to rise or fall depending hystoretically on the disposition of clay; the levitation by tiger waves is probably the same as by the steep waves discussed by Bai, Kelkar & Joseph (1996). The presence of steep tiger waves implies that long-wave theories like those leading to lubrication theory based on nonlinear perturbation theories or the Kuramoto and Sivaskinsky equations do not apply here. It was apparent to us that the loss of lubrication in the 25 mm pipe was associated with the formation of slugs; however, slugs may be lubricated. The linear stability analysis of core–annular flow does lead to predictions of the formation of shear stabilized slugs at low *Re* and the size of the slugs can be determined by using Rayleigh's selection criterion based on the wave length of the fastest growing wave (Bai, Chen & Joseph 1992); the case of self-lubricated bitumen froth should be similar. In larger pipes, like those which would be used in real pipelines, it is unlikely that capillary instability could take place; instead failure to stratified flow could be the mechanism which puts self-lubricated lines at risk to loss of lubrication at low speeds. Loss of lubrication at high speeds was not encountered in the experiments reported here. It is certain however that at very high-speed oil droplets will be pulled from wave crests and the transformation of the oil core with oil droplets of small sizes is a likely result. The main open questions for which guidance from the annular flow literature is not available concerns the liberation and absorption of water in self-lubrication and the effects of frictional heating on these properties.

This work was supported by the DOE, Department of Basic Energy Science, by the NSF, and by Syncrude, Canada. We wish to thank Taehwan Ko for taking the data presented in figures 7, 8 and 9.

REFERENCES

Bai, R., Chen, K. & Joseph, D. D. 1992 Lubricated pipelining: Stability of core–annular flow. Part 5. Experiments and comparison with theory. *J. Fluid Mech.* **240**, 97–142.

Bai, R., Kelkar, K. & Joseph, D. D. 1996 Direct simulation of interfacial waves in a high viscosity ratio and axisymmetric core annular flow. *Intl J. Multiphase Flow* **327**, 1–34.

Joseph, D. D., Bai, R., Chen, K. P. & Renardy, Y. 1997 Core-annular flows. *Ann. Rev. Fluid Mech.* **29**, 65–90.

Joseph, D. D. & Renardy, Y. 1992 *Fundamentals of Two-Fluid Dynamics.* Springer.

Kruka, V. 1977 Method for Establishing Core-Flow in Water-in-Oil Emulsions or Dispersions. Canadian Patent granted to Shell Canada Limited, No. 1008108.

Neiman, O. 1986 Froth pipelining tests. *Syncrude Canada Research and Development Progress Report* **15**(1), 373–407.

Reichardt, H. 1956 Uber die Geschwindigkeitsverteilung in einer geradlinigen turbulenten Couettestromung. *Z. Angew. Math. Mech. Sonderheft* S26–S29.

Yan, N. & Masliyah, J. H. 1994 Adsorption and desorption of clay particles at the oil–water interface. *J. Colloid Interface Sci.* **168**, 386.